

# The detection of neutrino interactions in the emulsion/lead target of the OPERA experiment

March 18, 2009

Submitted to JINST

N. Agafonova<sup>1</sup>, A. Anokhina<sup>2</sup>, S. Aoki<sup>3</sup>, A. Ariga<sup>4</sup>, T. Ariga<sup>4</sup>, L. Arrabito<sup>5</sup>, D. Autiero<sup>5</sup>, A. Badertscher<sup>6</sup>, A. Bagulya<sup>7</sup>, F. Bersani Greggio<sup>8</sup>, A. Bertolin<sup>9</sup>, M. Besnier<sup>10,a</sup>, D. Bick<sup>11</sup>, V. Boyarkin<sup>1</sup>, C. Bozza<sup>12</sup>, T. Brugière<sup>5</sup>, R. Brugnera<sup>13,9</sup>, G. Brunetti<sup>14,15</sup>, S. Buontempo<sup>16</sup>, E. Carrara<sup>13,9,b</sup>, A. Cazes<sup>5</sup>, L. Chaussard<sup>5</sup>, M. Chernyavsky<sup>7</sup>, V. Chiarella<sup>8</sup>, N. Chon-Sen<sup>17</sup>, A. Chukanov<sup>16</sup>, M. Cozzi<sup>14</sup>, G. D'Amato<sup>12</sup>, F. Dal Corso<sup>9</sup>, N. D'Ambrosio<sup>18</sup>, G. De Lellis<sup>19,16,c</sup>, Y. Déclais<sup>5</sup>, M. De Serio<sup>20</sup>, F. Di Capua<sup>16</sup>, D. Di Ferdinando<sup>15</sup>, A. Di Giovanni<sup>21</sup>, N. Di Marco<sup>21</sup>, C. Di Troia<sup>8</sup>, S. Dmitrievski<sup>22</sup>, A. Dominjon<sup>5</sup>, M. Dracos<sup>17</sup>, D. Duchesneau<sup>10</sup>, S. Dusini<sup>9</sup>, J. Ebert<sup>11</sup>, O. Egorov<sup>23</sup>, R. Enikeev<sup>1</sup>, A. Ereditato<sup>4</sup>, L. S. Esposito<sup>18</sup>, J. Favier<sup>10</sup>, G. Felici<sup>8</sup>, T. Ferber<sup>11</sup>, R. Fini<sup>20</sup>, D. Frekers<sup>24</sup>, T. Fukuda<sup>25</sup>, C. Fukushima<sup>26</sup>, V. I. Galkin<sup>2</sup>, V. A. Galkin<sup>27</sup>, A. Garfagnini<sup>13,9</sup>, G. Giacomelli<sup>14,15</sup>, M. Giorgini<sup>14,15</sup>, C. Goelnitz<sup>11</sup>, T. Goeltzenlichter<sup>17</sup>, J. Goldberg<sup>28</sup>, D. Golubkov<sup>23</sup>, Y. Gornushkin<sup>22</sup>, G. Grella<sup>12</sup>, F. Grianti<sup>8</sup>, M. Guler<sup>29</sup>, C. Gustavino<sup>18</sup>, C. Hagner<sup>11</sup>, T. Hara<sup>3</sup>, M. Hierholzer<sup>30</sup>, K. Hoshino<sup>25</sup>, M. Ieva<sup>20</sup>, K. Jakovcic<sup>31</sup>, B. Janutta<sup>11</sup>, C. Jollet<sup>17</sup>, F. Juget<sup>4</sup>, M. Kazuyama<sup>25</sup>, S. H. Kim<sup>35,d</sup>, M. Kimura<sup>26</sup>, B. Klicek<sup>31</sup>, J. Knuesel<sup>4</sup>, K. Kodama<sup>32</sup>, D. Kolev<sup>33</sup>, M. Komatsu<sup>25</sup>, U. Kose<sup>29</sup>, A. Krasnoperov<sup>22</sup>, I. Kreslo<sup>4</sup>, Z. Krumstein<sup>22</sup>, V.V. Kutsenov<sup>1</sup>, V.A. Kuznetsov<sup>1</sup>, I. Laktineh<sup>5</sup>, C. Lazzaro<sup>6</sup>, J. Lenkeit<sup>11</sup>, A. Ljubicic<sup>31</sup>, A. Longhin<sup>13</sup>, G. Lutter<sup>4</sup>, A. Malgin<sup>1</sup>, K. Manai<sup>5</sup>, G. Mandrioli<sup>15</sup>, A. Marotta<sup>16</sup>, J. Marteau<sup>5</sup>, V. Matveev<sup>1</sup>, N. Mauri<sup>14,15</sup>, F. Meisel<sup>4</sup>, A. Mereaglia<sup>17</sup>, M. Messina<sup>4</sup>, P. Migliozi<sup>16,\*</sup>, P. Monacelli<sup>21</sup>, K. Morishima<sup>25</sup>, U. Moser<sup>4</sup>, M. T. Muciaccia<sup>34,20</sup>, N. Naganawa<sup>25</sup>, M. Nakamura<sup>25</sup>, T. Nakano<sup>25</sup>, V. Nikitina<sup>2</sup>, K. Niwa<sup>25</sup>, Y. Nonoyama<sup>25</sup>, A. Nozdrin<sup>22</sup>, S. Ogawa<sup>26</sup>, A. Olchevski<sup>22</sup>, G. Orlova<sup>7</sup>, V. Osedlo<sup>2</sup>, D. Ossetski<sup>27</sup>, M. Paniccia<sup>8</sup>, A. Paoloni<sup>8</sup>, B. D Park<sup>25</sup>, I. G. Park<sup>35</sup>, A. Pastore<sup>34,20</sup>, L. Patrizii<sup>15</sup>, E. Pennacchio<sup>5</sup>, H. Pessard<sup>10</sup>, V. Pilipenko<sup>24</sup>, C. Pistillo<sup>4</sup>, N. Polukhina<sup>7</sup>, M. Pozzato<sup>14,15</sup>, K. Pretzl<sup>4</sup>, P. Publichenko<sup>2</sup>, F. Pupilli<sup>21</sup>, R. Rescigno<sup>12</sup>, D. Rizhikov<sup>27</sup>, T. Roganova<sup>2</sup>, G. Romano<sup>12</sup>, G. Rosa<sup>36</sup>, I. Rostovtseva<sup>23</sup>, A. Rubbia<sup>6</sup>, A. Russo<sup>19,16</sup>, V. Rzasny<sup>1</sup>, O. Ryazhskaya<sup>1</sup>, A. Sadoski<sup>22</sup>, O. Sato<sup>25</sup>, Y. Sato<sup>37</sup>, V. Saveliev<sup>27</sup>, A. Schembri<sup>36</sup>, W. Schmidt Parzefall<sup>11</sup>, H. Schroeder<sup>30</sup>, H. U. Schütz<sup>4</sup>, J. Schuler<sup>17</sup>, L. Scotto Lavina<sup>16</sup>, H. Shibuya<sup>26</sup>, S. Simone<sup>34,20</sup>, M. Sioli<sup>14,15</sup>, C. Sirignano<sup>12</sup>, G. Sirri<sup>15</sup>, J. S. Song<sup>35</sup>, M. Spinetti<sup>8</sup>, L. Stanco<sup>13</sup>, N. Starkov<sup>7</sup>, M. Stipcevic<sup>31</sup>, T. Strauss<sup>6</sup>, P. Strolin<sup>19,16</sup>, V. Sugonyaev<sup>13</sup>, S. Takahashi<sup>25</sup>, V. Tereschenko<sup>22</sup>, F. Terranova<sup>8</sup>, I. Tezuka<sup>37</sup>, V. Tioukov<sup>16</sup>, P. Tolun<sup>29</sup>, V. Tsarev<sup>7</sup>, R. Tsenov<sup>33</sup>, S. Tufanli<sup>29</sup>, N. Ushida<sup>32</sup>, V. Verguilov<sup>33</sup>, P. Vilain<sup>38</sup>, M. Vladimirov<sup>7</sup>, L. Votano<sup>8</sup>, J. L. Vuilleumier<sup>4</sup>, G. Wilquet<sup>38</sup>, B. Wonsak<sup>11</sup>, V. Yakushev<sup>1</sup>, C. S. Yoon<sup>35</sup>, Y. Zaitsev<sup>23</sup>, A. Zghiche<sup>10</sup>, and R. Zimmermann<sup>11</sup>.

1. INR-Institute for Nuclear Research of the Russian Academy of Sciences, RUS-117312 Moscow, Russia
2. SINP MSU-Skobeltsyn Institute of Nuclear Physics of Moscow State University, RUS-119992 Moscow, Russia
3. Kobe University, J-657-8501 Kobe, Japan

<sup>a</sup>Now at Laboratoire Leprince-Ringuet - École polytechnique, 91128 Palaiseau Cedex (France)

<sup>b</sup>Now at a private company

<sup>c</sup>Supported by travel fellowship from the School of Sciences and Technology – University of Naples Federico II

<sup>d</sup>Now at Chonnam National University

- 37 4. Centre for Research and Education in Fundamental Physics, Laboratory for High Energy Physics (LHEP), University of  
38 Bern, CH-3012 Bern, Switzerland  
39 5. IPNL, Université Claude Bernard Lyon 1, CNRS/IN2P3, F-69622 Villeurbanne, France  
40 6. ETH Zurich, Institute for Particle Physics, CH-8093 Zurich, Switzerland  
41 7. LPI-Lebedev Physical Institute of the Russian Academy of Sciences, RUS-117924 Moscow, Russia  
42 8. INFN - Laboratori Nazionali di Frascati dell'INFN, I-00044 Frascati (Roma), Italy  
43 9. INFN Sezione di Padova, I-35131 Padova, Italy  
44 10. LAPP, Université de Savoie, CNRS/IN2P3, F-74941 Annecy-le-Vieux, France  
45 11. Hamburg University, D-22761 Hamburg, Germany  
46 12. Dipartimento di Fisica dell'Università di Salerno and INFN, I-84084 Fisciano, Salerno, Italy  
47 13. Dipartimento di Fisica dell'Università di Padova, I-35131 Padova, Italy  
48 14. Dipartimento di Fisica dell'Università di Bologna, I-40127 Bologna, Italy  
49 15. INFN Sezione di Bologna, I-40127 Bologna, Italy  
50 16. INFN Sezione di Napoli, 80125 Napoli, Italy  
51 17. IPHC, Université de Strasbourg, CNRS/IN2P3, F-67037 Strasbourg, France  
52 18. INFN - Laboratori Nazionali del Gran Sasso, I-67010 Assergi (L'Aquila), Italy  
53 19. Dipartimento di Fisica dell'Università Federico II di Napoli, 80125 Napoli, Italy  
54 20. INFN Sezione di Bari, I-70126 Bari, Italy  
55 21. Dipartimento di Fisica dell'Università dell'Aquila and INFN, I-67100 L'Aquila, Italy  
56 22. JINR-Joint Institute for Nuclear Research, RUS-141980 Dubna, Russia  
57 23. ITEP-Institute for Theoretical and Experimental Physics, RUS-117259 Moscow, Russia  
58 24. University of Münster, D-48149 Münster, Germany  
59 25. Nagoya University, J-464-8602 Nagoya, Japan  
60 26. Toho University, J-274-8510 Funabashi, Japan  
61 27. Obninsk State University, Institute of Nuclear Power Engineering, RUS-249020 Obninsk, Russia  
62 28. Department of Physics, Technion, IL-32000 Haifa, Israel  
63 29. METU-Middle East Technical University, TR-06531 Ankara, Turkey  
64 30. Fachbereich Physik der Universität Rostock, D-18051 Rostock, Germany  
65 31. IRB-Rudjer Boskovic Institute, HR-10002 Zagreb, Croatia  
66 32. Aichi University of Education, J-448-8542 Kariya (Aichi-Ken), Japan  
67 33. Faculty of Physics, Sofia University "St. Kliment Ohridski", BG-1000 Sofia, Bulgaria  
68 34. Dipartimento di Fisica dell'Università di Bari, I-70126 Bari, Italy  
69 35. Gyeongsang National University, 900 Gazwa-dong, Jinju 660-300, Korea  
70 36. Dipartimento di Fisica dell'Università di Roma "La Sapienza" and INFN, I-00185 Roma, Italy  
71 37. Utsunomiya University, J-321-8505 Tochigi-Ken, Utsunomiya, Japan  
72 38. IIHE, Université Libre de Bruxelles, B-1050 Brussels, Belgium  
73 \*. Corresponding Author

## 74 Abstract

75 The OPERA neutrino detector in the underground Gran Sasso Laboratory (LNGS) was designed  
76 to perform the first detection of neutrino oscillations in appearance mode through the study of  $\nu_\mu \rightarrow \nu_\tau$   
77 oscillations. The apparatus consists of an emulsion/lead target complemented by electronic detectors  
78 and it is placed in the high energy long-baseline CERN to LNGS beam (CNGS) 730 km away from  
79 the neutrino source. Runs with CNGS neutrinos were successfully carried out in 2007 and 2008 with  
80 the detector fully operational with its related facilities for the emulsion handling and analysis. After a  
81 brief description of the beam and of the experimental setup we report on the collection, reconstruction  
82 and analysis procedures of first samples of neutrino interaction events.

## 83 1 Introduction

84 Neutrino oscillations were anticipated nearly 50 years ago [1] but they have been unambiguously observed only  
85 recently. Several experiments carried out in the last decades with atmospheric and accelerator neutrinos, as well  
86 as with solar and reactor neutrinos, contributed to our present understanding of neutrino mixing (see e.g. [2] for a  
87 review).

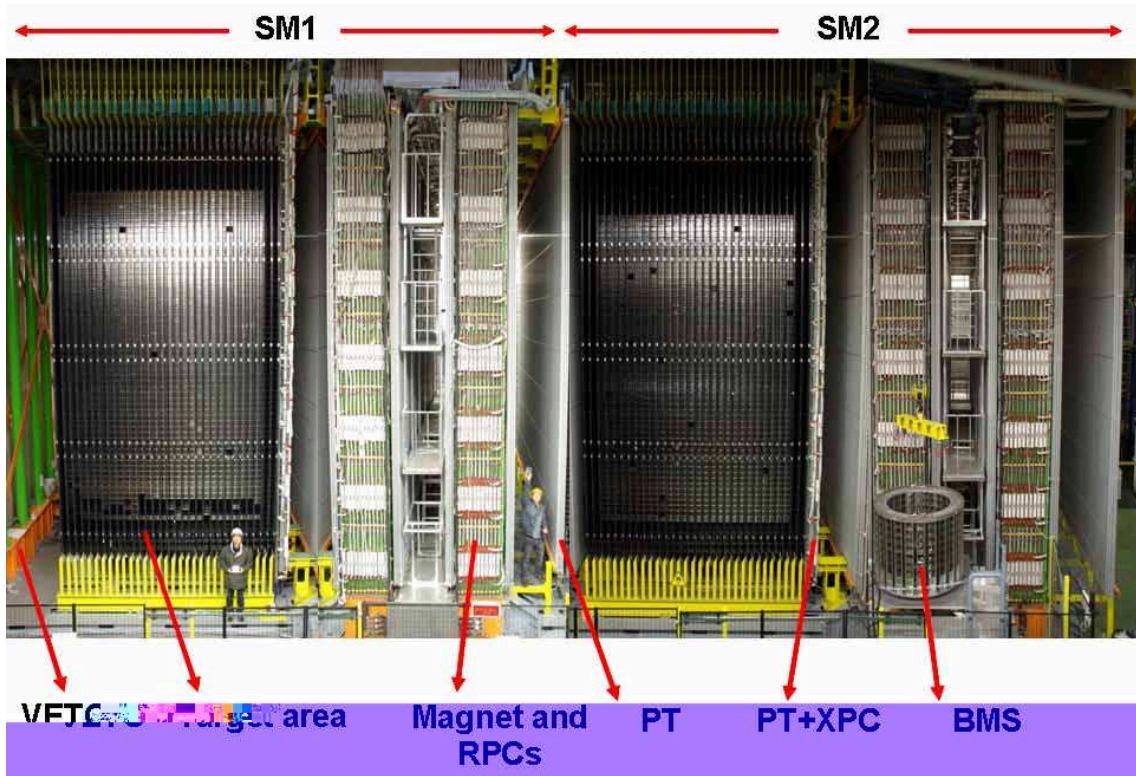


Figure 1: View of the OPERA detector. The upper horizontal lines indicate the position of the two identical supermodules (SM1 and SM2). The "target area" is made of walls filled with ECC bricks interleaved with planes of plastic scintillators (TT). Arrows show the position of the VETO planes, the drift tubes (PT) pulled alongside the XPC, the magnets and the RPC installed between the magnet iron slabs. The Brick Manipulator System (BMS) is also visible. See [6] for more details.

88 As far as the atmospheric neutrino sector is concerned, accelerator experiments can probe the same oscillation  
 89 parameter region as atmospheric neutrino experiments [3]. This is the case of the OPERA experiment that has the  
 90 main scientific task of the first direct detection of  $\nu_\mu \rightarrow \nu_\tau$  appearance, an important missing tile in the oscillation  
 91 scenario [4, 5, 6].

92 OPERA uses the long-baseline ( $L=730$  km) CNGS neutrino beam [7] from CERN to LNGS, the largest un-  
 93 derground physics laboratory in the world. The challenge of the experiment is to measure the appearance of  $\nu_\tau$   
 94 from  $\nu_\mu$  oscillations in an almost pure muon-neutrino beam. Therefore, the detection of the short-lived  $\tau$  lepton  
 95 ( $c\tau = 87.11 \mu\text{m}$ ) produced in the charged-current (CC) interaction of a  $\nu_\tau$  is mandatory. This sets two conflicting  
 96 requirements: a large target mass to collect enough statistics and an extremely high spatial accuracy to observe  
 97 the short-lived  $\tau$  lepton.

98 The  $\tau$  is identified by the detection of its characteristic decay topologies either in one prong (electron, muon  
 99 or hadron) or in three-prongs; its short track is measured with a large mass target made of 1 mm thick lead plates  
 100 (target mass and absorber material) interspaced with thin nuclear emulsion films (high-accuracy tracking devices).  
 101 This detector is historically called Emulsion Cloud Chamber (ECC). Among past applications it was successfully  
 102 used in the DONUT experiment for the first direct observation of the  $\nu_\tau$  [8].

103 OPERA is a hybrid detector made of two identical Super Modules (SM) each consisting of a target section of  
 104 about 625 tons made of emulsion/lead ECC modules (hereafter called "bricks"), of a scintillator tracker detector  
 105 (TT) needed to trigger the read-out and localize neutrino interactions within the target, and of a muon spectrometer  
 106 (Figure 1). The detector is equipped with an automatic machine (the Brick Manipulator System, BMS) that allows

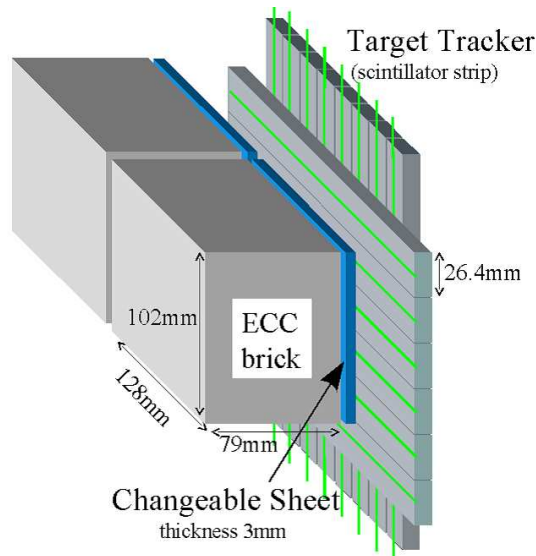


Figure 2: Schematic view of two bricks with their Changeable Sheets and target tracker planes.

107 the online removal of bricks from the detector. Ancillary, large facilities are used for the handling, the development  
 108 and the scanning of the emulsion films. Emulsion scanning is performed with two different types of automatic  
 109 microscopes: the European Scanning System (ESS) [9, 10] and the Japanese S-UTS [11].

110 A target brick consists of 56 lead plates of 1 mm thickness interleaved with 57 emulsion films [12]. The plate  
 111 material is a lead alloy with a small calcium content to improve its mechanical properties [13]. The transverse  
 112 dimensions of a brick are  $12.8 \times 10.2 \text{ cm}^2$  and the thickness along the beam direction is 7.9 cm (about 10 radiation  
 113 lengths). The bricks are housed in a light support structure placed between consecutive TT walls. More details on  
 114 the detector and on the ancillary facilities are given in [6].

115 In order to reduce the emulsion scanning load the use of Changeable Sheets (CS) film interfaces [14], successfully  
 116 applied in the CHORUS experiment [15], was extended to OPERA. Tightly packed doublets of emulsion films are  
 117 glued to the downstream face of each brick and can be removed without opening the brick. The global layout of  
 118 brick, CS and TT is schematically shown in Figure 2.

119 Charged particles from a neutrino interaction in the brick cross the CS and produce a signal in the TT  
 120 scintillators. The corresponding brick is then extracted and the CS developed and analyzed in the scanning  
 121 facilities at LNGS and in Nagoya. The information of the CS is then used for a precise prediction of the position  
 122 of the tracks in the most downstream films of the brick, hence guiding the *scan-back* vertex finding procedure.

123 A reconstructed CC event is shown in the bottom panels of Figure 3. In this case the detached event dimensions  
 124 are of the order of a few millimeters, to be compared with the  $\sim 10 \text{ m}$  scale of the whole event reconstructed with  
 125 the electronic detectors (top panels of Figure 3).

126 First neutrino data were collected by OPERA in 2006 [5] with the electronic detectors alone, and then in  
 127 2007 and 2008, for the first time with target bricks installed. All steps from the prediction of the brick where the  
 128 interaction occurred down to the kinematical analysis of the neutrino interactions are described in the following  
 129 using as benchmark a sub-sample of the statistics accumulated during the CNGS runs. The procedure has proven to  
 130 be successful. We are presently in the process of a quantitative evaluation of the different experimental efficiencies  
 131 that are involved in the analysis procedure, profiting of the increasing statistics of the reconstructed neutrino  
 132 events.

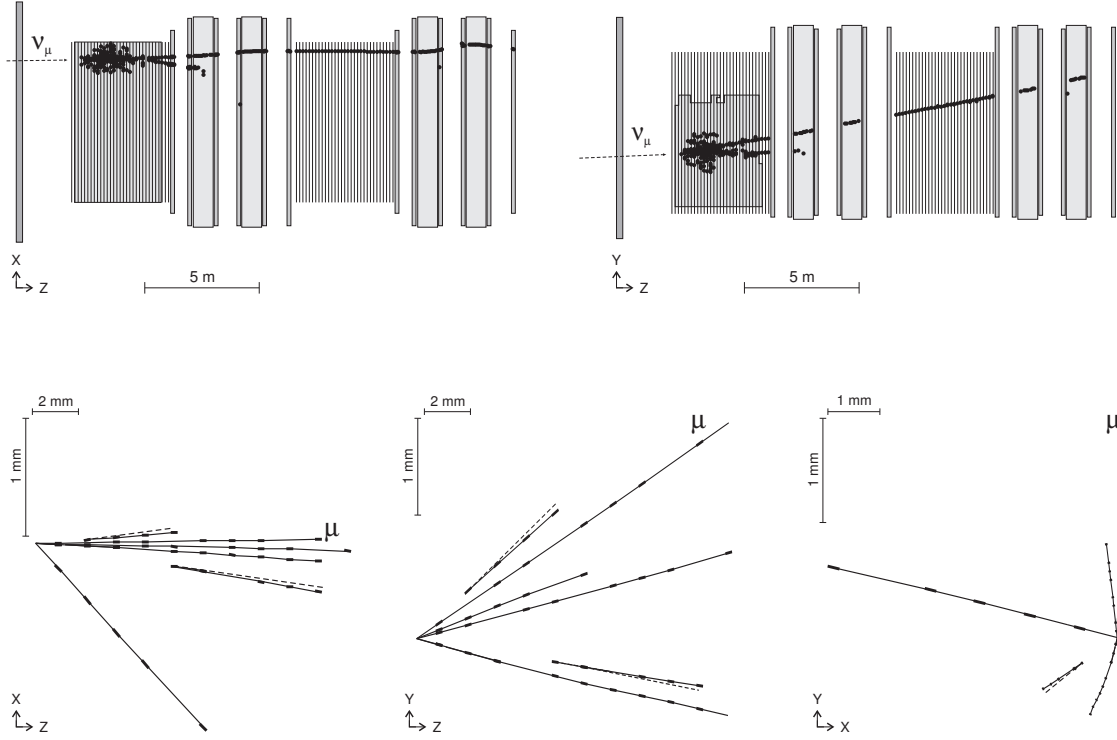


Figure 3: Top panels: on line display of an event seen by the OPERA electronic detectors (side and top views): a  $\nu_\mu$  interacts in one of the first bricks of the first supermodule (SM) yielding hadrons and a muon which is detected in both SMs and whose momentum is measured by the magnets of the two SMs. Bottom panels: the vertex of the same event observed in the emulsion films (side, top and front views). Note the two  $\gamma \rightarrow e^+e^-$  vertices: the opening angle between them is about 300 mrad. By measuring the energy of the  $\gamma$ 's one obtains a reconstructed invariant mass of  $110 \pm 30 \text{ MeV}/c^2$ , consistent with the  $\pi^0$  mass.

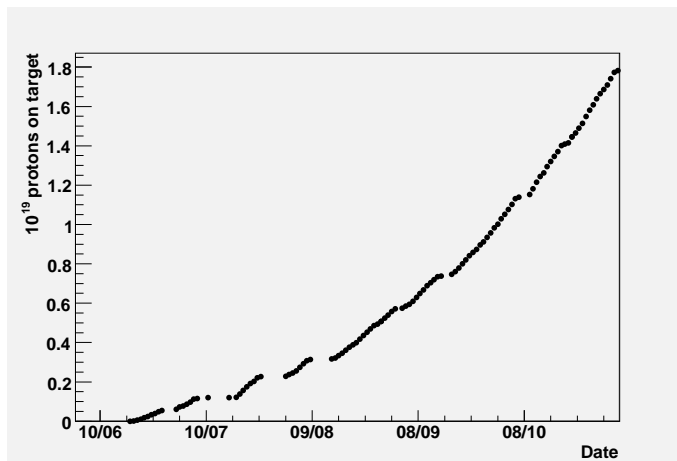


Figure 4: Integrated number of protons on target (p.o.t.) as a function of time for the 2008 CNGS run (June–November).

## 2 Real time detection of the CNGS Beam

The CNGS neutrino beam [7] was designed and optimized for the study of  $\nu_\mu \rightarrow \nu_\tau$  oscillations in appearance mode by maximizing the number of CC  $\nu_\tau$  interactions at the LNGS site. After a short commissioning run in 2006 the CNGS operation started on September 2007 at rather low intensity. The first event inside the OPERA target was observed on October 3<sup>rd</sup>. Unfortunately, due to a fault of the CNGS facility, the physics run lasted only a few days. During this run  $0.082 \times 10^{19}$  protons on target (p.o.t.) were accumulated with a mean value of  $1.8 \times 10^{13}$  protons per extraction<sup>a</sup>: this corresponds to about  $\sim 3.6$  effective nominal days of running. With such an integrated intensity 32 neutrino interactions in the bricks and 3 in the scintillator material of the target tracker were expected; we actually observed 38 events on time with the arrival of the beam at Gran Sasso.

A much longer run took place in 2008 when  $1.782 \times 10^{19}$  protons were delivered on the CNGS target. OPERA collected 10100 events on time and among them 1700 interactions in the bricks. The other events originated outside the target region (spectrometers, supporting structures, rock surrounding the cavern, hall structures, etc.). The run featured a poor initial efficiency of the CERN complex, with an average of about 40% until reaching an average value of about 60%. From October to November OPERA gathered the same number of events as from June to August. The 2008 CNGS integrated p.o.t. intensity as a function of time is shown in Figure 4.

During the 2007 and 2008 runs all electronic detectors were operational and the live time of the data acquisition system exceeded 99%. More than 10 million events were collected by applying a minimum bias filter. The selection of beam related events relies upon a time stamp, based on the time synchronization accuracy of 100 ns between the CERN beam GPS tagging and the OPERA timing system.

An automatic classification algorithm provides high efficiency in the selection of neutrino interactions inside the OPERA target both for CC and neutral-current (NC) events at the expenses of a slight contamination of neutrino interactions in the external material.

For the early 2007 run the algorithm selected 53 events occurring inside the target while expecting 50; the contamination from neutrino interactions outside the target amounted to 37% (Monte Carlo simulation). The low purity of the selected event sample was due to some sub-detectors still being in the commissioning phase and to the OPERA target that was only partially filled with bricks. In the 2008 run 1663 events were classified as interactions in the target (expected 1723) with a contamination from outside events of only 7%.

The muon momentum distribution for events classified as CC interactions in the target is shown in the left panel of Figure 5. The distribution of the muon angle with respect to the horizontal axis is shown in the right

<sup>a</sup>The 400 GeV proton beam is extracted from the CERN SPS in two  $10.5 \mu\text{s}$  pulses, with design intensity of  $2.4 \times 10^{13}$  p.o.t.

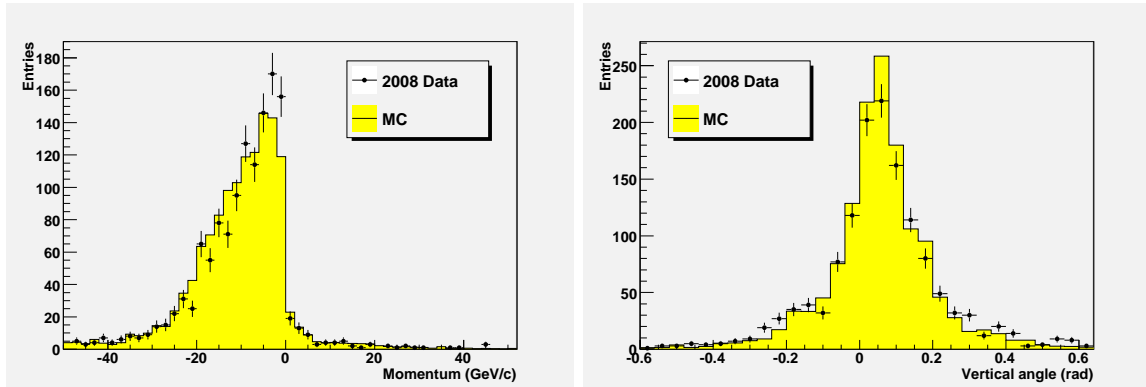


Figure 5: Left: momentum distribution of muons produced in CC neutrino interactions inside the OPERA target. Right: angular distribution of the muon tracks with respect to the horizontal axis.

162 panel of Figure 5; the beam direction angle is found to be tilted by 58 mrad, as expected from geodesy.

163 An extensive study of the beam monitoring is being performed by using neutrino interactions both in the whole  
 164 OPERA detector and in the surrounding rock material. This will be the subject of a forthcoming publication.

### 165 3 Combined analysis of electronic detectors and nuclear emulsion film 166 data

167 We describe in the following the breakdown of the different steps carried out to analyze neutrino interaction events  
 168 from the identification of the "fired" brick up to the detailed kinematical analysis of the vertex in the emulsion  
 169 films.

170 Once a trigger in the electronic detectors is selected to be compatible with an interaction inside a brick the  
 171 following procedure is applied [6]:

- 172 1. electronic detector data are processed by a software reconstruction program that selects the brick with the  
 173 highest probability to contain the neutrino interaction vertex;
- 174 2. this brick is removed from the target wall by the BMS and exposed to X-rays for film-to-film alignment.  
 175 There are two independent X-ray exposures: the first one ensures a common reference system to the CS film  
 176 doublet and the most downstream film of the brick (frontal exposure); the second one produces thick lateral  
 177 marks on the brick edges, used for internal alignment and film numbering within the brick;
- 178 3. after the first X-ray exposure the CS doublet is detached from the brick and developed underground, while  
 179 the brick is kept in a box made of 5 cm thick iron shielding to reduce the radioactivity background;
- 180 4. if the CS scanning detects tracks compatible with those reconstructed in the electronic detectors the second  
 181 X-ray exposure (lateral marking) is performed and the brick is brought to the surface laboratory. The brick  
 182 is then exposed to cosmic-rays for about 24 hours in a dedicated pit in order to select high-energy cosmic  
 183 muons to provide straight tracks for a refined (sub-micrometric) film-to-film alignment;
- 184 5. the brick emulsion films are then developed and dispatched to the various scanning laboratories in Europe  
 185 and Japan.

186 The procedure described above has proven to be successful. As an example, in Figure 6 we show the number of  
 187 bricks extracted by the BMS per week, about one hundred. This is matched by the 100 CS developed and scanned  
 188 per week in the LNGS (Italy) and Tono (Japan) scanning stations.



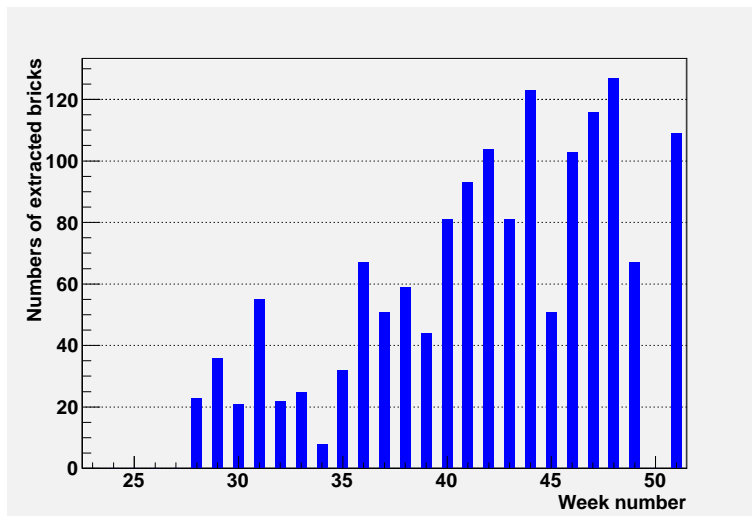


Figure 6: The number of bricks extracted per week by the BMS in 2008.

189 Brick Finding and Changeable Sheet Interplay

190 The efficiency for selecting the "fired" brick is the convolution of several effects and measurements. Here we  
 191 discuss the two most important ones, the Brick Finding procedure and the Changeable Sheet measurement, for  
 192 which preliminary results have been obtained from the analysis of partial samples of already scanned events.

193 The brick finding algorithm exploits the tracking capabilities of the OPERA electronic detectors and, by  
 194 combining this information with the output of a Neural Network for the selection of the most probable wall where  
 195 the interaction occurred, provides a list of bricks with the associated probability that the interaction occurred  
 196 therein. A preliminary estimate of the brick finding efficiency, limited to the extraction of the first most probable  
 197 brick (for about 700 events) and not considering the small fraction ( $< 5\%$ ) of events for which the present electronic  
 198 detector reconstruction fails, is compatible with the Monte Carlo estimate of 70% computed for a standard mixture  
 199 of CC and NC events. A higher efficiency can be obtained by extracting also bricks ranked with lower probabilities.

200 The tracking efficiency of single emulsion films can be measured by an exposure to high-energy pion beams  
 201 and amounts to about 90% [10]. However, the measurement of the CS doublet efficiency in situ, in the OPERA  
 202 detector, is by far more challenging, given the coarse resolution in the extrapolation of tracks from the electronic  
 203 detectors to the CS.

204 At present, we are studying the CS tracking efficiency by two independent approaches: (a) all tracks produced  
 205 in already located neutrino vertices are followed downstream and searched for in the corresponding CS doublet;  
 206 (b) muon tracks reconstructed by the electronic detectors and found in the CS are properly normalized to the total  
 207 number of CC events where at least one track (not necessarily the muon) is found in the CS. The two methods  
 208 yield a preliminary efficiency for finding a track in both films of the CS doublet which is compatible with the  
 209 conservative expectation of 90% on a single film [10]. The experimental efficiency has been evaluated on a sample  
 210 of 100 events scanned in both the European and the Japanese laboratories. We are presently working in order to  
 211 further increase this efficiency by employing more advanced analysis techniques.

212 Vertex analysis

213 All tracks measured in the CS are sought in the most downstream films of the brick and followed back until  
 214 they are not found in three consecutive films. The stopping point is considered as the signature either for a primary  
 215 or a secondary vertex. The vertex is then confirmed by scanning a volume with a transverse size of 1 cm<sup>2</sup> for 11  
 216 films in total, upstream and downstream of the stopping point (see Figure 7). Preliminary estimates of the vertex  
 217 location efficiency are in agreement with the Monte Carlo expectations of 90% and 80% for CC and NC events,  
 218 respectively. This evaluation has been performed on a sample of 500 located events.



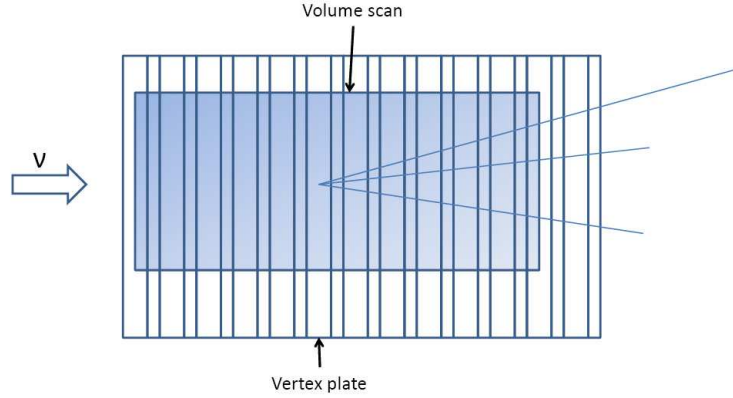


Figure 7: Schematic view of the volume scan performed around the stopping point of the track.

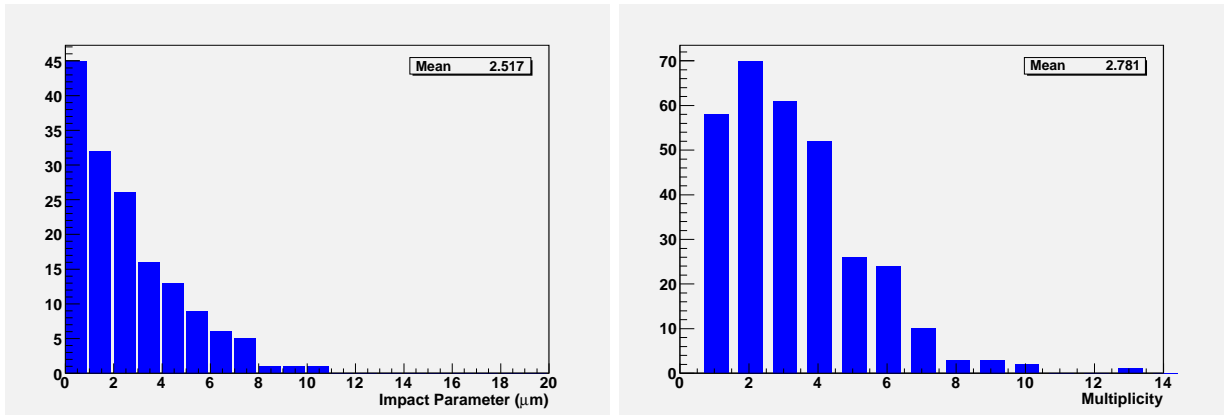


Figure 8: Left panel: impact parameter distribution of the muon track in CC events with respect to the reconstructed vertices. Right panel: charged track multiplicity distribution of the events.

219 The track impact parameter distribution of the muon in CC events with respect to the reconstructed vertex  
 220 position and the event track multiplicity distribution are shown in Figure 8. As expected, the impact parameter  
 221 distribution is peaked at zero and has a mean value of  $2.5 \mu\text{m}$ . The multiplicity distribution shows the anticipated  
 222 enhancements for even track numbers due to the preferred interaction of neutrinos with neutrons.

223 As an example, in Figures 9 and 10 we show a NC and a CC event, respectively, fully reconstructed in the  
 224 brick. A very "peculiar" event is shown in Figure 11: the neutrino interaction occurred in the bottom layer of an  
 225 emulsion film. Therefore, the associated nuclear fragments (large angle heavy ionizing tracks) are also visible in  
 226 the film containing the vertex.

### 227 Decay topologies

228 Charm production and decay topology events have a great importance in OPERA for two main reasons. On  
 229 the one hand in order to certify the observation of  $\tau$  events one should prove the ability of observing charm events  
 230 at the correct expected rate. On the other hand, since charm decays exhibit the same topology as  $\tau$  decays, they  
 231 are a potential source of background if the muon at the primary vertex is not identified (see Figure 12). Therefore,  
 232 searching for charm-decays in events with the primary muon correctly identified provides a direct measurement of  
 233 this background.

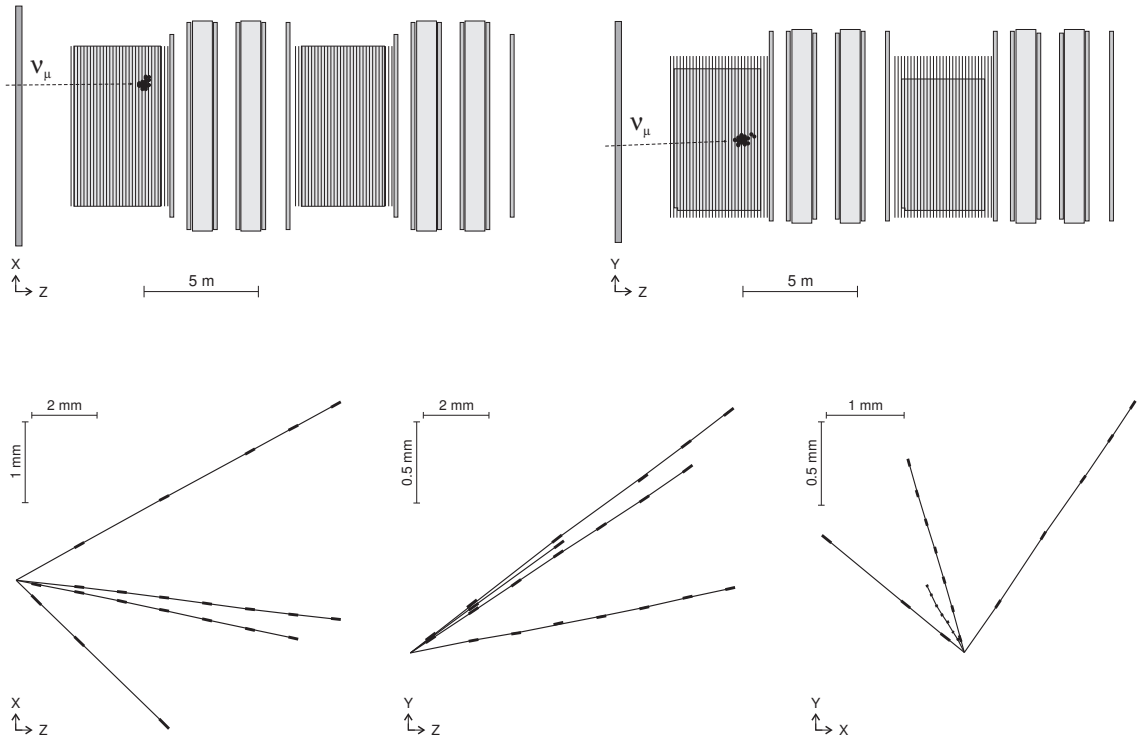


Figure 9: Top panels: online display of one NC event seen by the OPERA electronic detectors. The regions filled with bricks are highlighted. Bottom panels: the emulsion reconstruction is shown in the bottom panels: top view (bottom left), side view (bottom center), front view (bottom right).

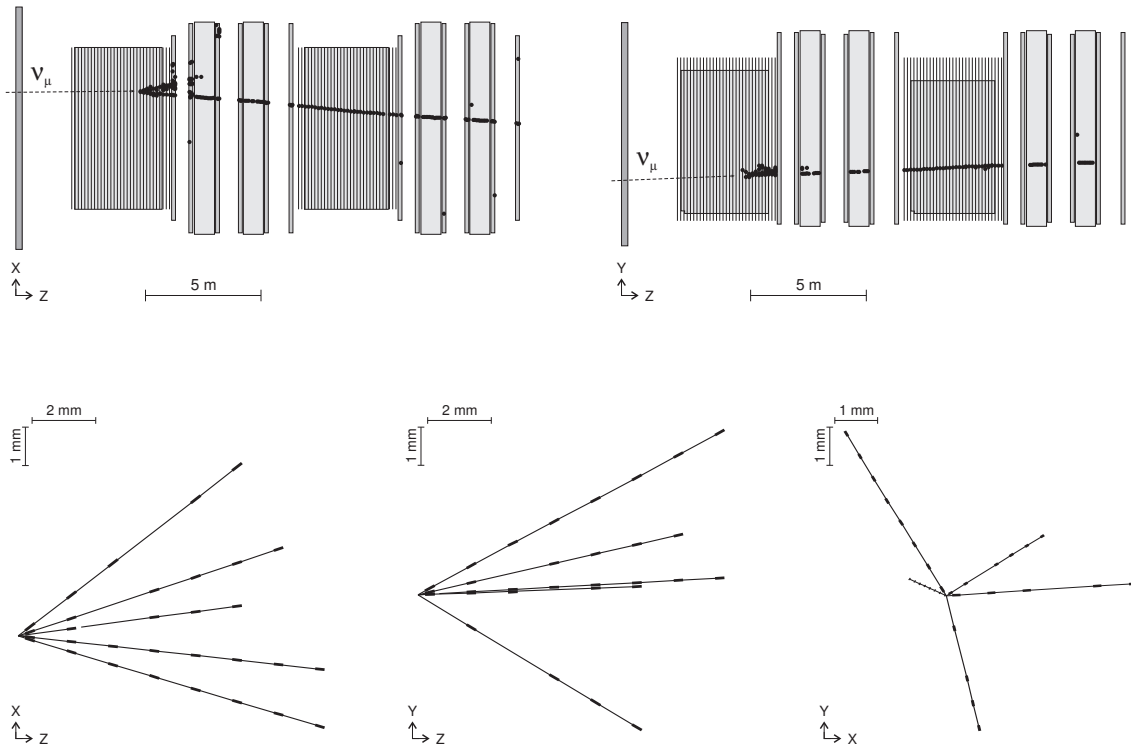


Figure 10: Top panels: online display of one CC event seen by the OPERA electronic detectors. Bottom panels: the emulsion reconstruction is shown in the bottom panels: top view (bottom left), side view (bottom center), front view (bottom right).

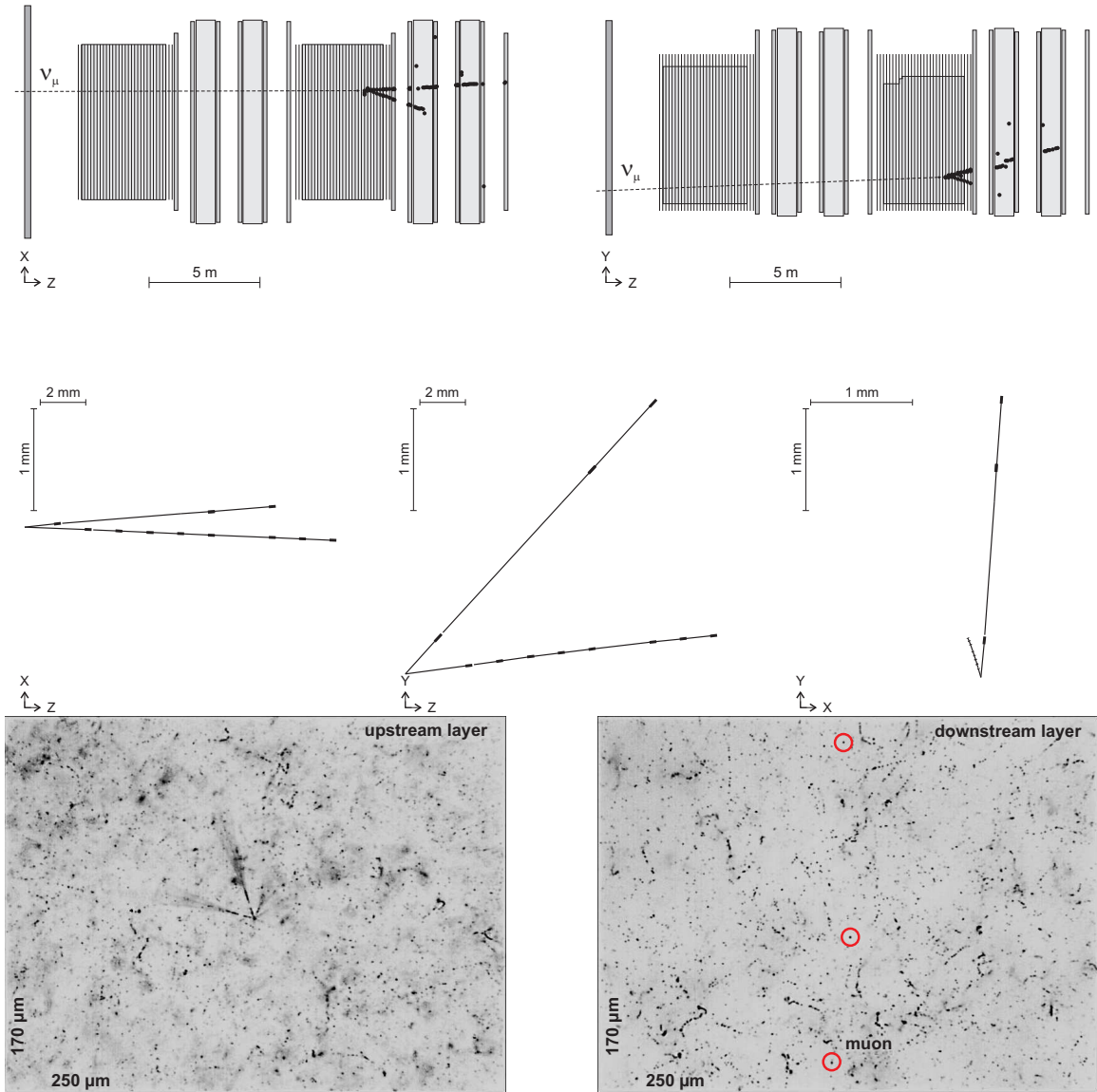


Figure 11: Display of the OPERA electronic detector of a  $\nu_\mu$  CC interaction, top and side views. The emulsion reconstruction is shown in the middle panels: top view (bottom left), side view (bottom center), frontal view (bottom right). Bottom left panel : picture of the interaction vertex as seen by the microscope CMOS camera. The nuclear fragments produced in the interaction are visible. Bottom right panel : picture taken about 200 micron far from the interaction vertex. The minimum ionizing particles produced in the interaction are indicated by a circle. The muon track is also indicated.

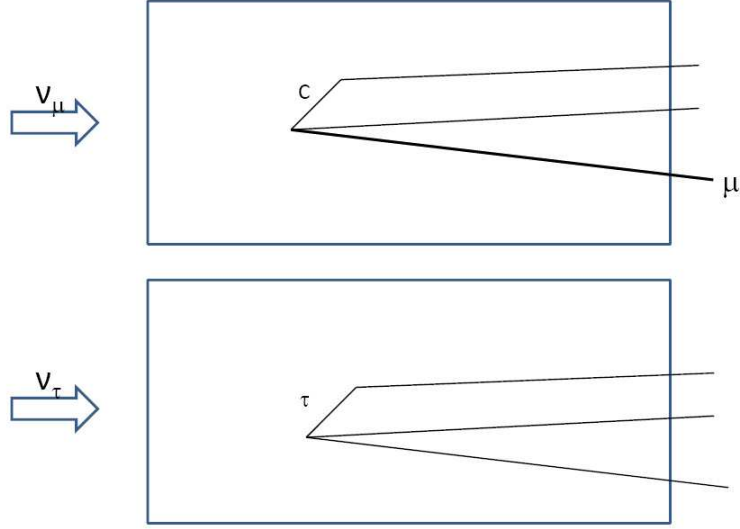


Figure 12: Schematic view of the charm and tau decay topologies.

234 Charm decay topologies were searched for in the sample of located neutrino interactions. Two events with  
 235 charm-like topologies were found. By using the neutrino-induced charm-production cross-section measured by the  
 236 CHORUS experiment [17] about 3 charged-charm decays are expected to be observed in the analyzed sample.

237 The event in Figure 13 has high track multiplicity at the primary vertex and one of the scan-back tracks shows  
 238 a kink topology. The measured decay angle is 204 mrad and the flight length of the decaying particle is 3247  $\mu\text{m}$ .  
 239 The decay occurred in the third lead plate downstream of the interaction plate. No large angle tracks are produced  
 240 at the decay vertex. This allows to further rule out the hadronic interaction hypothesis. The muon track and the  
 241 charm candidate track lie in a back-to-back configuration ( $\Delta\phi \simeq 165^\circ$ ) as one would expect for charm production.  
 242 The daughter momentum, measured by using the Multiple Coulomb Scattering technique is  $3.9_{-0.9}^{+1.7}$  GeV/c at the  
 243 90% C.L. Therefore, at the 90% C.L. the transverse momentum ranges between 600 MeV/c and 1150 MeV/c, well  
 244 above the cut of 250 MeV/c applied to reject hadronic decays. According to the FLUKA Monte Carlo [18] the  
 245 probability that a hadron interaction mimics a charm-decay with transverse momentum larger than 600 MeV/c is  
 246 only  $4 \times 10^{-4}$ .

247 The second charm-like topology is shown in Figure 14. A 4-prong primary vertex is observed originating at a  
 248 depth of about 30  $\mu\text{m}$  in the upstream lead plate. The charmed hadron track points to a 3-prong decay vertex  
 249 located at a distance of 1150  $\mu\text{m}$  from the primary vertex (200  $\mu\text{m}$  inside the lead). All tracks have a clear CS tag.  
 250 The interaction occurs downstream in the brick and the tracks only cross four emulsion films and the CS doublet  
 251 (the two most downstream hits in the figure). The muon track and the charm candidate track lie in a back-to-back  
 252 configuration ( $\Delta\phi \simeq 150^\circ$ ). The relativistic  $\gamma$  of the charmed parent has been roughly estimated as the inverse of  
 253 the average angle in space that the daughter tracks form with it. This leads to a  $\gamma$  value of about 8.6, implying a  
 254 parent high momentum of  $\sim 16$  GeV/c (assuming the  $D^+$  mass). The momenta of the daughter tracks have also  
 255 been measured by extracting the downstream brick and using the Multiple Coulomb Scattering technique. The  
 256 measured values are  $p_1=2.4_{-0.6}^{+1.3}$ ,  $p_2=1.3_{-0.3}^{+0.4}$  and  $p_3=1.2_{-0.4}^{+1.7}$  GeV/c (transverse momenta of about 610, 90 and  
 257 340 MeV/c, total momentum:  $4.8_{-0.8}^{+2.2}$  GeV/c), at the 90% C.L. The probability of a hadron interaction has been  
 258 evaluated using FLUKA and amounts to  $10^{-6}$ . Assuming a  $D \rightarrow K\pi\pi$  decay, an invariant mass of  $1.1_{-0.1}^{+0.2}$  GeV/c<sup>2</sup>  
 259 is obtained. On the other hand assuming a  $D_s \rightarrow KK\pi$  decay an invariant mass of  $1.5_{-0.1}^{+0.4}$  GeV/c<sup>2</sup> is derived. In  
 260 the latter case the invariant mass is consistent with the mass of a charmed hadron while in the second case the  
 261 consistency is marginal. The probability of a decay in flight of a  $K$  is about  $10^{-3}$ .

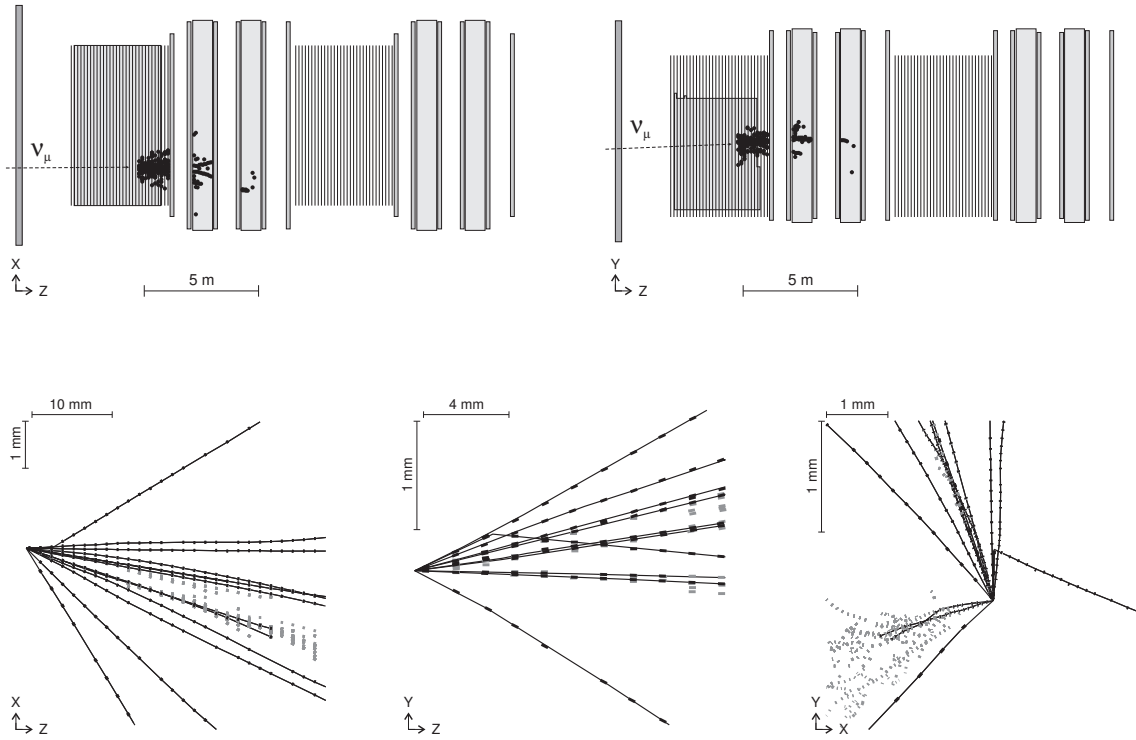


Figure 13: Online display of the OPERA electronic detector of a  $\nu_\mu$  charged-current interaction with a charm-like topology (top panel). The emulsion reconstruction is shown in the bottom panels where the charm-like topology is seen as a track with a kink: top view (bottom left), side view (bottom center), frontal view (bottom right).

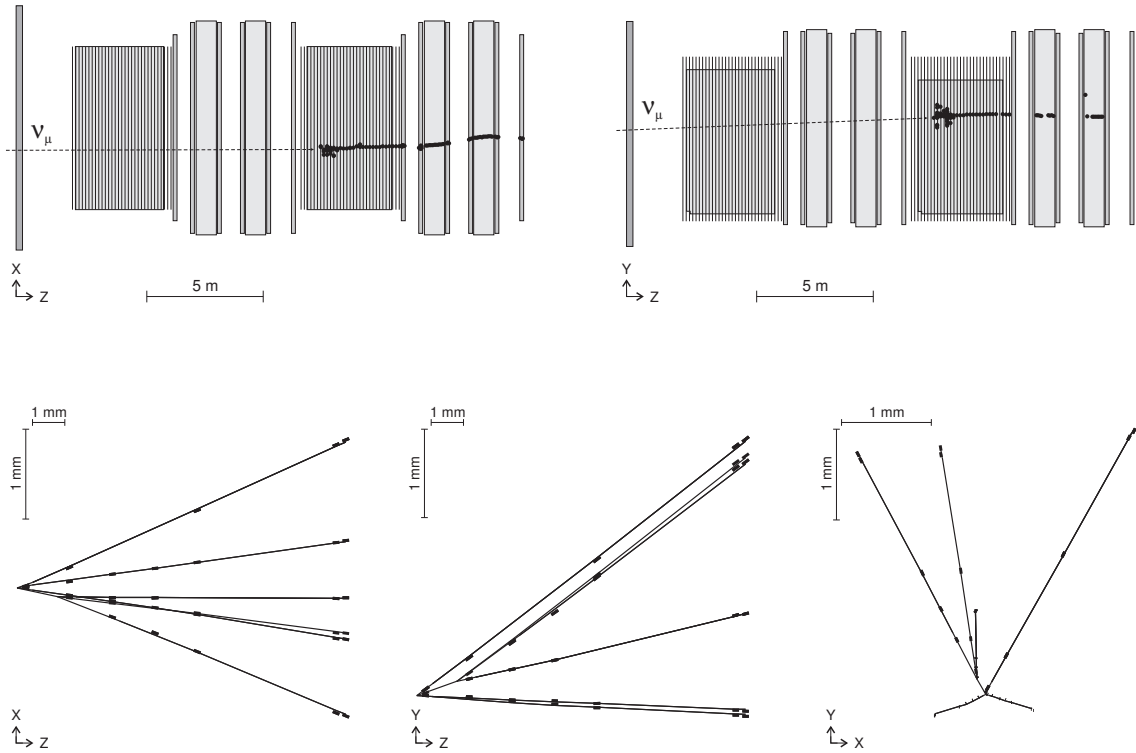


Figure 14: Online display of the OPERA electronic detector of a  $\nu_\mu$  charged-current interaction with a charm-like topology (top panel). The emulsion reconstruction is shown in the bottom panels where the charm-like topology is seen as a three-prongs secondary vertex: top view (bottom left), side view (bottom center), frontal view (bottom right).



## 262 4 Conclusions

263 The 2007 and 2008 CNGS runs constitute an important milestone for the LNGS OPERA experiment searching for  
264  $\nu_\mu \rightarrow \nu_\tau$  oscillations. First samples of neutrino interaction events have been collected in the emulsion/lead target  
265 and allowed to check the complete analysis chain starting from the trigger down to the neutrino vertex location in  
266 the emulsions and to the topological and kinematical characterization of the event.

267 In this paper we reported on the capability in performing an online identification, extraction and development  
268 of the bricks where the neutrino interaction occurred, vertex location and kinematical reconstruction. The overall  
269 performance of the experiment during the running phase and through the analysis chain can be summarized by  
270 stating that:

- 271 • all electronic detectors performed excellently allowing the precise localization of the brick hit by the neutrino;
- 272 • the electronic detector event reconstruction was tuned to the brick finding procedure which operated for the  
273 first time with real neutrino events providing good results;
- 274 • all experimental activities from brick removal upon identification to the X and cosmic-ray exposures, brick  
275 disassembly and emulsion development, have been successfully accomplished. At present more than 100  
276 bricks per week can be routinely handled;
- 277 • the scanning of the Changeable Sheets can be performed with the expected detection efficiencies;
- 278 • vertex location was successfully attempted for both CC and NC events;
- 279 • the topological and kinematical analyses of the vertices were successfully exploited and led to an unambiguous  
280 interpretation of neutrino interactions. In particular two events with a charm-like topology were found so  
281 far in the analyzed sample. This is fully consistent with expectations based on the known neutrino-induced  
282 charm production cross-section.

283 The above considerations make us confident that the OPERA experiment is definitely in its production phase  
284 with the CNGS beam and that the scene has been set for the discovery of the  $\tau$  appearance.  
285

## 286 5 Acknowledgements

287 We thank CERN for the commissioning of the CNGS facility and for its successful operation, and INFN for  
288 the continuous support given to the experiment during the construction, installation and commissioning phases  
289 through its LNGS laboratory. We warmly acknowledge funding from our national agencies: Fonds de la Recherche  
290 Scientifique - FNRS and Institut Interuniversitaire des Sciences Nucleaires for Belgium, MoSES for Croatia, IN2P3-  
291 CNRS for France, BMBF for Germany, INFN for Italy, the Japan Society for the Promotion of Science (JSPS),  
292 the Ministry of Education, Culture, Sports, Science and Technology (MEXT) and the Promotion and Mutual Aid  
293 Corporation for Private Schools of Japan for Japan, SNF and ETH Zurich for Switzerland, the Russian Foundation  
294 for Basic Research (grants 08-02-91005 and 08-02-01086) for Russia, the Korea Research Foundation Grant (KRF-  
295 2007-013-C00015) for Korea. We are also indebted to INFN for providing fellowships and grants to non Italian  
296 researchers. Finally, we are indebted to our technical collaborators for the excellent quality of their work over many  
297 years of design, prototyping and construction of the detector and of its facilities.

## 298 References

- 299 [1] B. Pontecorvo, Sov. Phys. JETP **6**, 429 (1957);  
300 B. Pontecorvo, Sov. Phys. JETP **7**, 172 (1958);  
301 Z. Maki, M. Nakagawa and S. Sakata, Prog. Theor. Phys. **28**, 870 (1962).
- 302 [2] A. Strumia and F. Vissani, “Neutrino masses and mixings and...,” arXiv:hep-ph/0606054.

- 303 [3] K. S. Hirata *et al.* [KAMIOKANDE-II Collaboration], Phys. Lett. B **205**, 416 (1988);  
304 Y. Fukuda *et al.* [Super-Kamiokande Collaboration], Phys. Rev. Lett. **81**, 1562 (1998);  
305 J. Hosaka *et al.* [Super-Kamiokande Collaboration], Phys. Rev. D **74**, 032002 (2006);  
306 K. Abe *et al.* [Super-Kamiokande Collaboration], Phys. Rev. Lett. **97** 171801 (2006);  
307 S. P. Ahlen *et al.* [MACRO Collaboration], Phys. Lett. B **357**, 481 (1995);  
308 M. Ambrosio *et al.* [MACRO Collaboration], Phys. Lett. B **434**, 451 (1998);  
309 M. Ambrosio *et al.* [MACRO Collaboration], Eur. Phys. J. C **36**, 323 (2004);  
310 W. W. M. Allison *et al.* [SOUDAN2 Collaboration], Phys. Lett. B **449**, 137 (1999);  
311 W. W. M. Allison *et al.* [SOUDAN2 Collaboration], Phys. Rev. D **72**, 052005 (2005);  
312 M. H. Ahn *et al.* [K2K Collaboration], Phys. Rev. D **74**, 072003 (2006);  
313 D.G. Michael *et al.* [MINOS Collaboration], Phys. Rev. Lett. **97** 191801 (2006);  
314 P. Adamson *et al.* [MINOS Collaboration], Phys. Rev. Lett. **101** 221804 (2008).
- 315 [4] A. Ereditato, K. Niwa and P. Strolin, INFN-AE-97-06, DAPNU-97-07, Jan 1997;  
316 H. Shibuya *et al.* [OPERA Collaboration], LNGS-LOI-8-97;  
317 M. Guler *et al.*, CERN-SPSC-2000-028.
- 318 [5] R. Acquafredda *et al.* [OPERA Collaboration], New J. Phys. **8** 303 (2006).
- 319 [6] R. Acquafredda *et al.* [OPERA Collaboration] "The OPERA experiment in the CERN to Gran Sasso neutrino  
320 beam", submitted to JINST.
- 321 [7] CNGS project: <http://proj-cngs.web.cern.ch/proj-cngs/>.
- 322 [8] K. Kodama *et al.* [DONUT Collaboration], Phys. Lett. B **504**, 218 (2001).
- 323 [9] G. Rosa *et al.*, Nucl. Instrum. Meth. A **394**, 357 (1997);  
324 N. Armenise *et al.*, Nucl. Instrum. Meth. A **551**, 261 (2005);  
325 M. De Serio *et al.*, Nucl. Instrum. Meth. A **554**, 247 (2005);  
326 L. Arrabito *et al.*, Nucl. Instrum. Meth. A **568** 578 (2006);  
327 I. Kreslo *et al.*, JINST **3** (2008) P04006.
- 328 [10] L. Arrabito *et al.*, JINST **2** P05004 (2007).
- 329 [11] S. Aoki *et al.*, Nucl. Instrum. Meth. B **51**, 466 (1990);  
330 T. Nakano, PhD Thesis, University of Nagoya (1997);  
331 T. Nakano [CHORUS Collaboration], *International Europhysics Conference on High-Energy Physics (HEP*  
332 *2001)*, Budapest, Hungary, 12-18 July 2001.
- 333 [12] T. Nakamura *et al.*, Nucl. Instrum. Meth. A **556**, 80 (2006).
- 334 [13] A. Anokhina *et al.* [OPERA Collaboration], JINST **3** P07002 (2008).
- 335 [14] A. Anokhina *et al.* [OPERA Collaboration], JINST **3** P07005 (2008).
- 336 [15] E. Eskut *et al.* [CHORUS Collaboration], Nucl. Instrum. Meth. A **401**, 7 (1997).
- 337 [16] M. De Serio *et al.*, Nucl. Instrum. Meth. **A512** (2003) 539;  
338 K. Kodama *et al.*, Nucl. Instrum. Meth. **A574** (2007) 192.
- 339 [17] F. Di Capua, "10th International Workshop on Neutrino Factories, Super beams and Beta beams", Valencia-  
340 Spain, June 30 - July 5 2008. Proceedings available at <http://pos.sissa.it/cgi-bin/reader/conf.cgi?confid=74>
- 341 [18] For details on the FLUKA Monte Carlo we refer to <http://www.fluka.org>